Laboratory Investigation (2017) 97, 1008–1019

Roflumilast reverses polymicrobial sepsis-induced liver damage by inhibiting inflammation in mice

Hongfang Feng, Jiajia Chen, Haitao Wang, Yufang Cheng, Zhengqiang Zou, Qiuping Zhong and Jiangping Xu

Sepsis is a life-threatening syndrome accompanied by an overwhelming inflammatory response and organ dysfunction. Selective targeting of phosphodiesterase 4 (PDE4) is currently being investigated as an effective therapeutic approach for inflammation-associated diseases. Roflumilast is a selective PDE4 inhibitor, used for the treatment of severe chronic obstructive pulmonary disease in clinic. However, its role in the treatment of sepsis-induced liver damage remains unclear. In the present study, we evaluated the effects of roflumilast in mice with cecal ligation and puncture-induced sepsis, and investigated the underlying mechanism. We found that roflumilast treatment improved survival in septic mice by reducing bacterial load locally and systemically, inhibiting the expression of pro-inflammatory cytokines interleukin-6 and tumor necrosis factor alpha, and alleviating liver injury. These effects were associated with the inhibition of nuclear translocation of nuclear factor-kappa B (NF-κB), as well as degradation of NF-κB inhibitory protein alpha. The phosphorylation of p38 mitogen-activated protein kinase (MAPK) was also markedly inhibited by roflumilast. Moreover, roflumilast significantly suppressed the activation of signal transducer and activator of transcription 3 (STAT3) and its upstream Janus kinase 1 and Janus kinase 2. Taken together, these results indicate that roflumilast prevents polymicrobial sepsis likely by suppressing NF-κB, p38 MAPK, and STAT3 pathways.

Laboratory Investigation (2017) **97,** 1008–1019; doi:10.1038/labinvest.2017.59; published online 26 June 2017

Sepsis is a dysregulated host response to infection, resulting in life-threatening organ dysfunction and even high mortality rates.[1,2] Sepsis affects one-third of all the patients on admission or during the intensive care unit stay, with a mortality estimated at 25–35%.[3–5] In addition to the impact on patients, sepsis accounted for approximately US$ 24 billion of total hospital costs in the United States.[6] The pathophysiology of sepsis and advances in medical care are clearly established. However, pharmaceutical studies failed to result in any substantial progress in drug design, development, or therapy.[7] Novel treatment options for sepsis are imperative in view of the significant morbidity and mortality correlated with sepsis, and the limited advances in pharmaceutical interventions.

The systemic inflammatory response syndrome is initiated by rapid infection following injury. The dysregulated systemic response leads to multiple organ dysfunction syndrome characterized by liver, pulmonary, cardiovascular, renal, and gastrointestinal dysfunction, and death.[1] In particular, sepsis-associated liver dysfunction and failure are closely correlated with high mortality. It is reported in patients with sepsis that the incidence of sepsis-associated liver dysfunction and hepatic failure ranged from 34 to 46%, and from 1.3 to 22%, respectively.[8,9] The absence of resolution of baseline hepatic dysfunction or the development of hepatic dysfunction in the first week of sepsis was associated with a lower 28-day survival rate.[10] Furthermore, the persistence or development of liver failure within the 72 h period after the onset of severe sepsis was strongly associated with poor outcome in French.[11] Therefore, the outcome of sepsis may be improved by relieving liver injury.

Several cytokines are secreted during sepsis, which are correlated with the severity of the condition.[12] Tumor necrosis factor alpha (TNF-α) and interleukin-6 (IL-6) are the major inflammatory mediators that are significantly elevated in sepsis.[12,13] The liver has a major role in the pathogenesis of sepsis, either as a tissue source for these cytokines or as the target organ of these mediators mediating liver injury.[14] Excessive generation of cytokines is regulated by the activation of several signaling pathways, such as nuclear factor-kappa B (NF-κB) and p38 mitogen-activated protein kinase (MAPK).[14–16] The NF-κB-binding activity, degradation

Neuropharmacology and Drug Discovery Group, School of Pharmaceutical Sciences, Southern Medical University, Guangzhou, China
Correspondence: Professor J Xu, MD, PhD, Neuropharmacology and Drug Discovery Group, School of Pharmaceutical Sciences, Southern Medical University, 1838 Guangzhou Avenue North, Guangzhou 510515, China.
E-mail: jpx@smu.edu.cn

Received 1 November 2016; revised 27 April 2017; accepted 27 April 2017

of NF-κB inhibitory protein (IκB), and nuclear accumulation of the NF-κB are enhanced during sepsis.[17,18] Prevention of NF-κB activation suppresses the production of inflammatory cytokines and liver injury.[19] Moreover, cytokines exhibit their biological effects associated with liver injury via activation of complex signaling cascades. The Janus kinase–signal transducer and activator of transcription (JAK–STAT) pathway is an essential pathway mediating the signal transduction of cytokines such as IL-6, IL-10, and interferon alpha in the pathogenesis of sepsis.[20,21] Inhibition of JAK–STAT pathway relieves sepsis-induced liver injury.[20] Thus, suppression of excessive generation of cytokines and related signaling pathways may constitute a valid therapeutic strategy for sepsis-induced liver injury.

Phosphodiesterase 4 (PDE4) is an intracellular enzyme that catalyzes the hydrolysis of adenosine 3′,5′-cyclic monophosphate (cAMP), thereby regulating its downstream signaling. It is well known that PDE4 inhibitors prevent the degradation of cAMP and elevate cAMP-response element-binding protein (CREB) phosphorylation, leading to enhanced biological effects.[22] PDE4 inhibitors have previously been reported to significantly inhibit inflammatory response in various disease models, such as chronic obstructive pulmonary disease (COPD), asthma, psoriatic arthritis, and Alzheimer's disease.[23] Moreover, recent studies have suggested that PDE4 inhibitors have beneficial effects in experimental liver injury, including bile duct ligation-induced liver injury, alcoholic liver injury, and T-cell-mediated liver failure.[24–26] These evidences demonstrate that PDE4 inhibitors can prevent inflammation response and alleviate liver injury, which are two important aspects in the pathogenesis of sepsis. Roflumilast is the first PDE4 inhibitor approved by the United States Food and Drug Administration (US FDA) for the treatment of COPD, with a significant anti-inflammation effects and potential protective effects on organ injury.[27,28] Thus, we are interested to investigate the role of roflumilast in sepsis. In the present study, we delineated the possible effects of roflumilast in mice with cecal ligation and puncture (CLP)-induced sepsis and to identify the involved signaling pathways.

MATERIALS AND METHODS

Reagents and Antibodies

Roflumilast was purchased from Sigma-Aldrich (St Louis, MO, USA). The Aspartate Aminotransferase Assay Kit and the Alanine Aminotransferase Assay Kit were purchased from Jiancheng Bioengineering Institute (Nanjing, China). The Mouse TNF-α ELISA Kit and the Mouse IL-6 ELISA Kit were purchased from Boster (Wuhan, China). The Mouse/Rat cAMP Parameter Assay Kit was purchased from R&D (Minneapolis, MN, USA). The Nuclear and Cytoplasmic Protein Extraction Kit was purchased from Beyotime (Jiangsu, China). Antibodies against IL-6, TNF-α, CREB, phospho-CREB, phospho-JAK1, phospho-JAK2, phospho-STAT3, NF-κB p65, phospho-p38 MAPK, p38 MAPK, and Histone H3 were purchased from Cell Signaling Technology (Danvers, MA, USA). Antibodies against IκB-α, JAK1, JAK2, and STAT3 were purchased from Abgent (San Diego, CA, USA). Antibodies against GAPDH was purchased from Abcam (Cambridge, MA, USA).

Animals

Male C57BL/6 mice (6–8 weeks old) weighing 20 ± 2 g each were obtained from the Animal Resource Center of Southern Medical University (Guangzhou, China). Mice were housed in a specific pathogen-free animal facility under controlled environmental conditions of 22 ± 2 °C and a 12 h light–dark cycle, with a standard pellet diet and water *ad libitum*. All the protocols were approved by the Institutional Animal Care and Use Committee of Southern Medical University, in accordance with the Guide for the Care and Use of Laboratory Animals of the National Institutes of Health.

Pharmacological Treatments

Roflumilast was dissolved in dimethyl sulfoxide and diluted in 0.5% carboxymethyl cellulose sodium (CMC) to final concentrations. Mice were randomly divided into five groups: sham-operated group treated with 0.5% CMC; CLP group exposed to 0.5% CMC; CLP plus a low-dose roflumilast group receiving 0.3 mg/kg body weight roflumilast; CLP plus a middle dose roflumilast group treated with 1.0 mg/kg body weight roflumilast; and CLP plus a high-dose roflumilast group receiving 3.0 mg/kg body weight roflumilast. Roflumilast or vehicle was administered orally by gavage with a gastric tube once daily for 7 consecutive days before CLP surgery.

CLP-Induced Sepsis

CLP was performed as described previously.[13,29] Briefly, the peritoneal cavity was opened under isoflurane anesthesia. The cecum was exteriorized and tightly ligated at the designated distal end of the ileo-cecal valve using a non-absorbable 6-0 suture. The cecum was thoroughly perforated once with a 21-gauge needle. After removing the needle, small droplets of feces were extruded from the perforation sites. The cecum was returned into the peritoneal cavity and the incision was closed in layers with a 6-0 suture. Mice in sham-operated group followed exactly the same procedures except for the ligation and puncture. Mice were resuscitated by injecting 1 ml of pre-warmed saline subcutaneously.

Survival Study

In the survival study, mice were subjected to CLP or sham operation. Mice were pre-treated with roflumilast orally once daily for 7 consecutive days. The degree of sepsis was evaluated by the presence of piloerection, suppressed spontaneous activity, slow or no response to touch and auditory stimuli, hunch, conjunctivitis, and dyspnea.[30,31] The clinical signs were scored from 0 to 4. The total score was calculated by adding the individual scores in every item, resulting in a maximum score of 28. Dead mice were scored

on the basis of the highest clinical observations.[31] Mice were monitored for 7 days after the induction of sepsis.

Bacterial Count

At 24 h after CLP, mice were killed, and the whole blood was drawn from the orbital plexus into heparinized tubes. For peritoneal lavage, 3 ml of sterile PBS was injected into and aspirated from the abdominal cavity three times, after aseptic preparation of the abdominal wall.[31] Livers were aseptically collected, individually weighed, and homogenized in sterile PBS using a tissue homogenizer. After serial log dilutions of whole blood, peritoneal lavage fluid, and liver homogenates, 100 μl of each dilution was plated on tryptic soy agar.[31] After incubation at 37 °C for 24 h, bacterial colonies were counted and expressed as log CFU/ml blood or peritoneal lavage fluid, and log CFU/g tissue.

Enzyme-Linked Immunosorbent Assay

For cytokine measurements, plasma was obtained from whole blood samples after centrifugation at 3000 r.p.m. for 15 min at 4 °C. Peritoneal lavage fluid was collected in 3×3 ml of PBS, followed by centrifugation at 3000 r.p.m. for 15 min at 4 °C to remove cell debris. Livers were homogenized with five volumes of ice-cold lysis buffer containing 50 mM Tris, 150 mM NaCl, 1% Triton X-100, 1 mM PMSF, a protease inhibitor cocktail, and a phosphatase inhibitor cocktail, and centrifuged at 10 000 r.p.m. for 5 min at 4 °C. IL-6 and TNF-α in supernatants were measured using enzyme-linked immunosorbent assay (ELISA) kits according to the respective manufacturer's instructions. The data were expressed as pg/ml peritoneal lavage fluid or blood, or pg/mg protein. The protein concentrations were determined using a BCA protein assay kit (Pierce, Rockford, IL, USA).

Biochemical Analysis

Plasma levels of alanine aminotransferase (ALT) and aspartate aminotransferase (AST), expressed as U/l, were measured using commercially available assay kits according to the respective manufacturer's instructions.

Histological Study

Liver samples from each group were excised 24 h post CLP and fixed in 10% formalin for 24 h. The fixed livers were paraffin-embedded, cut coronally at 4 μm, and stained with hematoxylin and eosin (H&E). The images were recorded via bright-field microscopy using a Nikon Eclipse Ti-U (Tokyo, Japan). Swollen hepatocytes, polymorphonuclear neutrophil (PMN) infiltration, central vein congestion, and sinusoidal congestion were determined as previously described.[32,33]

cAMP Assay

Livers were collected 24 h post CLP, rinsed with PBS, and homogenized in ice-cold 0.1 mol/l HCL lysis buffer at a 1:5 ratio (w/v). Particulates were removed by centrifugation at 6000 *g* for 10 min at 4 °C, and the supernatant was neutralized with 0.1 mol/l NaOH. The cAMP levels were measured using Mouse/Rat cAMP Parameter Assay Kit.

Western Blot

Western blot was performed as described previously.[34] Livers were excised 24 h after CLP. Proteins of each sample were extracted in ice-cold lysis buffer and the concentrations were detected using a BCA protein assay kit. A unit of 30 μg of total protein per sample were subjected to 10 or 12% SDS-PAGE and electrophoretically transferred onto a PVDF membrane. The membrane was incubated with 5% (w/v) skim milk in Tris-buffered saline with Tween-20 for 2 h at room temperature, and incubated overnight at 4°C with different primary antibodies. Subsequently, the membrane was washed three times, and incubated with goat-anti-rabbit IgG-HRP secondary antibody for 1 h at room temperature. After washing, immunoreactive bands were visualized using Immobilon Western Chemiluminescent HRP Substrate (Millipore, Boston, MA, USA). The densitometry of bands was quantified using the Image J software. GAPDH was used as control protein for blots on total protein and on the cytoplasmic fraction, and Histone H3 was used for blots on the nuclear fraction.

Subcellular Fractionation

Nuclear and cytoplasmic fractions of livers from all the mice were isolated as described previously.[34] In brief, tissues were homogenized in ice-cold buffer A followed by the addition of 1 mM DTT, 1 mM PMSF, and protease inhibitors, and incubated on ice for 10 min. Tissues were lysed with buffer B, vortexed vigorously for 5 s, and incubated on ice for 1 min. After centrifugation at 16 000 r.p.m. for 5 min at 4 °C, the supernatants (cytoplasmic extract) were transferred. Precipitates were resuspended in buffer C followed by the addition of 1 mM DTT, 1 mM PMSF, and protease inhibitors, vortexed for 15 s, and incubated on ice for 30 min with intermittent vortexing for 15 s every 10 min. The supernatants (nuclear extract) were recovered after centrifugation at 16000 r.p.m. for 10 min at 4 °C.

Statistics

All the statistical analyses were performed using SPSS software (SPSS, Chicago, IL, USA), and graphs were drawn using GraphPad Prism 5.01 (GraphPad, La Jolla, CA, USA). The survival curves and mean survival time were determined using the Kaplan–Meier method and analyzed with a log-rank test. Bacterial results were expressed as medians, and other results were expressed as mean ± s.e.m. The groups were compared using ANOVA followed by Bonferroni test or Kruskal–Wallis test followed by Dunnett's test, where appropriate. Differences were considered significant at $P < 0.05$.

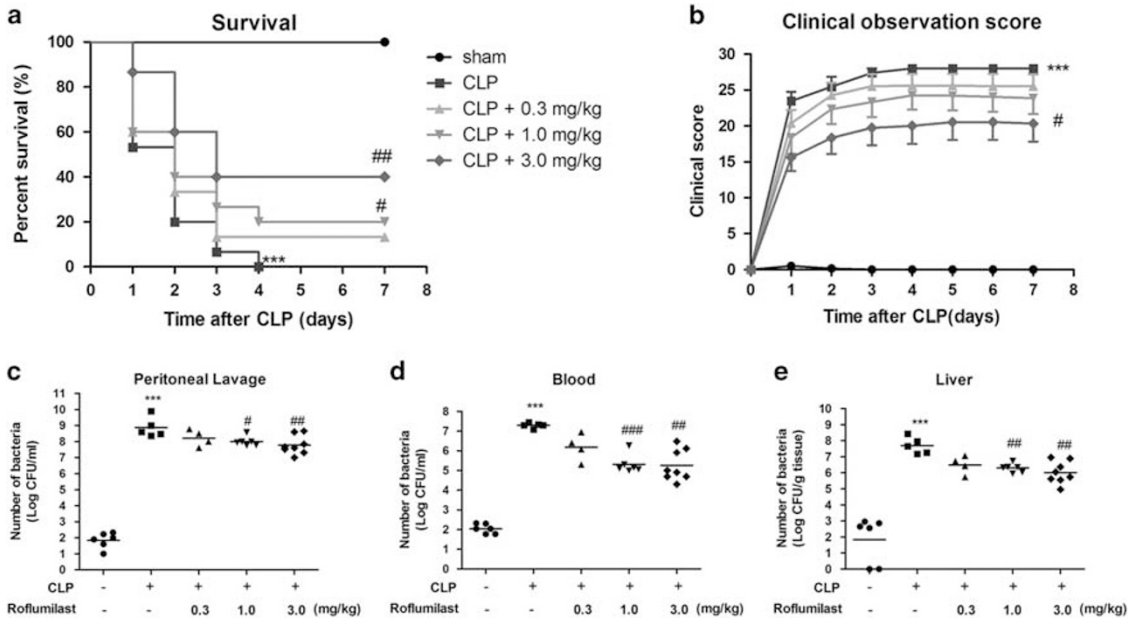

Figure 1 Roflumilast improved survival and reduced bacterial load in CLP-induced sepsis. (**a**) Mice were subjected to CLP or sham operation. Sham group, $n=6$; other groups, $n=15$. The survival was monitored for 7 days after surgery. (**b**) The clinical signs were scored for 7 days after surgery. Data were expressed as mean ± s.e.m. (**c**–**e**) Mice were subjected to CLP or sham operation. Sham group, $n=6$; other groups, $n=12$. Peritoneal lavage fluid, blood, and livers were collected 24 h after surgery. Bacterial counts were determined after 24 h incubation. Data were expressed as medians and compared using Kruskal–Wallis. $^{***}P<0.001$, compared with sham group; $^{\#}P<0.05$, $^{\#\#}P<0.01$, $^{\#\#\#}P<0.001$, compared with CLP group.

RESULTS

Roflumilast Improved Survival in CLP-Induced Sepsis

Severe sepsis is a major cause of mortality. Therefore, we performed an experimental randomized controlled animal study to investigate the survival rate of mice subjected to CLP-induced sepsis, and the impact of roflumilast pre-treatment on sepsis. We conducted an observational study in mice during 7 days after CLP surgery. The mean survival time of septic mice in CLP group was 1.80 ± 0.24 days. Roflumilast pre-treatment at a dose of 3.0 and 1.0 mg/kg body weight significantly increased the survival time to 4.07 ± 0.64 days and 2.87 ± 0.58 days, respectively, compared with that of the CLP group. Pre-treatment with roflumilast at a dose of 0.3 mg/kg body weight improved the survival time to 2.47 ± 0.50 days. All the sham mice survived during the 7 days of observation (Figure 1a).

The CLP mice demonstrated a rapidly increasing symptom score after surgery and showed the highest values compared with the sham-operated group. Pre-treatment with roflumilast at a dose of 0.3 and 1.0 mg/kg body weight induced symptoms shortly after CLP showing a relatively lower score. Symptoms were delayed and improved significantly in mice treated with 3.0 mg/kg body weight roflumilast compared with the CLP group (Figure 1b). These data suggest that roflumilast improves survival and relieves clinical signs of septic mice.

Roflumilast Reduced Bacterial Load in CLP-Induced Sepsis

Local bacterial load and systemic bacterial dissemination are the central events triggering dysregulated host response during CLP-induced sepsis.[35] Therefore, we measured the CFU of bacteria in the peritoneal fluid, blood, and liver in septic mice. CLP mice displayed substantially higher levels of live bacterial load compared with sham mice. Treatment with roflumilast at a dose of 1.0 and 3.0 mg/kg body weight substantially reduced the bacterial load in peritoneal fluid compared with the CLP treatment (Figure 1c). Moreover, blood and hepatic bacterial loads were markedly lower in mice treated with roflumilast at a dose of 1.0 and 3.0 mg/kg body weight (Figures 1d and e). These data demonstrate that the protective effects of roflumilast are possibly related to the clearance of bacteria from the site of infection and the prevention of systemic bacterial dissemination.

Roflumilast Decreased Cytokine Levels in CLP-Induced Sepsis

An overwhelming inflammatory response due to cytokine storm is a major cause of organ dysfunction and death in sepsis.[36] Therefore, we evaluated the effects of roflumilast on the accumulation of pro-inflammatory cytokines IL-6 and TNF-α. Levels of IL-6 (Figures 2a and b) and TNF-α (Figures 2d and e) were greatly enhanced in the peritoneal cavity and plasma of septic mice compared with sham mice. Roflumilast administration markedly decreased TNF-α and IL-6 levels compared with CLP mice. These data indicate that roflumilast improves survival of septic mice by suppressing cytokine generation.

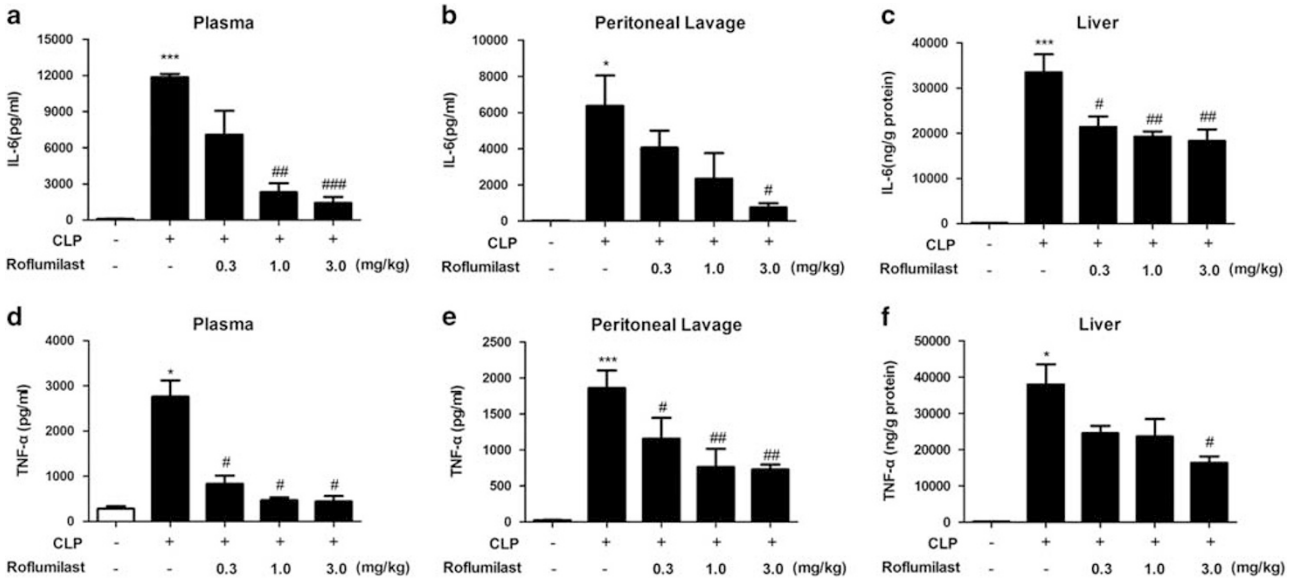

Figure 2 Roflumilast decreased cytokine levels in CLP-induced sepsis. Mice were subjected to CLP or sham operation. Sham group, $n=6$; other groups, $n=12$. Peritoneal lavage fluid, plasma, and livers were collected 24 h after surgery. (**a**–**c**) The levels of IL-6 in the peritoneal lavage fluid, plasma, and livers were determined by ELISA. (**d**–**f**) The levels of TNF-α in the peritoneal lavage fluid, plasma, and livers were determined by ELISA. Data were expressed as mean ± s.e.m. and compared using ANOVA. $^{*}P<0.05$, $^{***}P<0.001$, compared with sham group; $^{\#}P<0.05$, $^{\#\#}P<0.01$, $^{\#\#\#}P<0.001$, compared with CLP group.

Roflumilast Inhibited Liver Inflammation and Dysfunction

One of the major consequences of sepsis is the development of liver dysfunction.[8,9] Roflumilast may inhibit liver inflammation and damage. We determined the concentrations of pro-inflammatory cytokines TNF-α and IL-6 in liver. Pretreatment with roflumilast significantly reduced TNF-α and IL-6 levels in liver homogenates compared with the levels in CLP group (Figures 2c and f). Furthermore, we measured plasma levels of AST and ALT as indicators of hepatocellular injury. In CLP mice, we found strongly elevated plasma levels of AST and ALT, when compared with sham mice, and roflumilast treatment significantly reduced their levels (Figures 3b and c). The effect of roflumilast-mediated protection was further confirmed by evaluating liver sections. In the livers of CLP mice, sepsis increased PMN infiltration, hepatocytes swelling, and central vein and sinusoidal congestion. Roflumilast treatment decreased the incidence of these changes, protecting mice against sepsis-induced liver damage (Figure 3a). These data show that roflumilast suppresses inflammatory response in liver and ameliorates liver injury caused by sepsis.

Roflumilast Elevated cAMP Accumulation and CREB Phosphorylation in CLP-Induced Sepsis

Roflumilast, as a PDE4 inhibitor, activated the cAMP–CREB pathway, resulting in an anti-inflammation.[22] Thus, we measured the cAMP levels in liver homogenates to determine the efficacy of roflumilast treatment after CLP. Our results showed that roflumilast elevated the intracellular cAMP levels and CREB phosphorylation at Ser133 in septic mice. Notably, the levels of cAMP and phosphorylated CREB greatly declined in untreated sepsis (Figure 4). Moreover, consistent with the ELISA results, roflumilast reduced TNF-α and IL-6 levels in liver, which was further confirmed by western blot (Figures 5a–c).

Roflumilast Inhibited IκB Degradation, NF-κB Nuclear Translocation, and p38 MAPK Phosphorylation in CLP-Induced Sepsis

TLR-mediated NF-κB and p38 MAPK signaling pathways have important roles in inflammatory response and are activated in sepsis.[15,37] Activation of NF-κB correlates with the phosphorylation, ubiquitination, and degradation of IκB. NF-κB translocates to the nucleus where it initiates transcription of immune-related genes.[37] As no differences in NF-κB p65 expression were detected among the groups (Figures 6a and c), we examined the degradation of IκB, which regulates the activity of NF-κB. We found that CLP-induced sepsis led to downregulation of IκB-α, whereas administration of roflumilast to septic mice significantly inhibited the degradation (Figures 6a and b). Furthermore, the nuclear translocation of NF-κB p65 was significantly increased after CLP, and this increase was strongly abrogated by roflumilast treatment (Figures 7a–d). In parallel, roflumilast significantly decreased the level of phosphorylated p38 MAPK (Figures 6a and d).

Roflumilast Inhibited STAT3 Signaling in CLP-Induced Sepsis

It is known that cytokines utilize the activation of complex signaling cascades to exert biological effects. As IL-6 is a

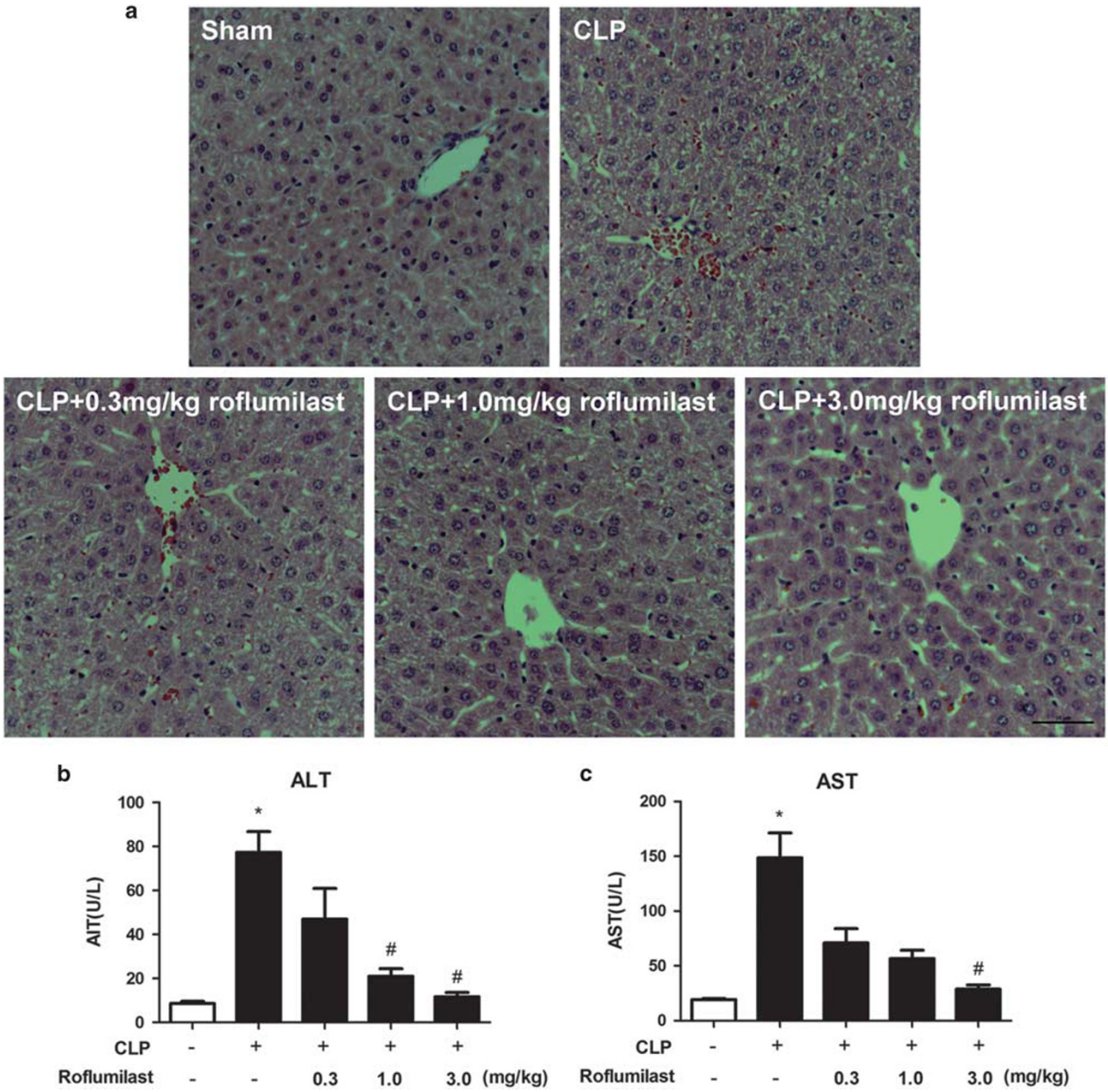

Figure 3 Roflumilast alleviated liver damage in CLP-induced sepsis. (**a**) Livers were collected 24 h after CLP or sham operation. Liver histological sections were stained with H&E. The original amplification was ×400. Bar = 50 μm. (**b**, **c**) Mice were subjected to CLP or sham operation. Sham group, $n = 6$; other groups, $n = 12$. Plasma was collected 24 h after surgery. The levels of ALT and AST in plasma were determined. Data were expressed as mean ± s.e.m. and compared using ANOVA. $^{*}P < 0.05$, compared with sham group; $^{\#}P < 0.05$, compared with CLP group.

known upstream activator of STAT3 signaling, we investigated the role of STAT3 in sepsis, and in turn evaluated the potential effect of roflumilast on STAT3. No changes in STAT3 expression were observed in any group (Figures 8a and e). We then measured the phosphorylation of STAT3 at the residue important for DNA-binding activity (Tyr705) or at the site required for maximal transcriptional activity (Ser727).[38,39] Our results showed that CLP mice exhibited higher STAT3 Tyr705 phosphorylation than sham mice, which was inhibited by roflumilast treatment (Figures 8a and d). No differences in phosphorylated Ser727 were detected among groups (not shown). To further investigate the molecular mechanisms underlying roflumilast-induced STAT3 inhibition, we determined JAK1 and JAK2 phosphorylation. We found that roflumilast treatment significantly decreased the phosphorylation of JAK1 and JAK2 in septic mice (Figures 8a–c), indicating that the decrease in STAT3 phosphorylation was dependent, at least in part, on JAK1 and

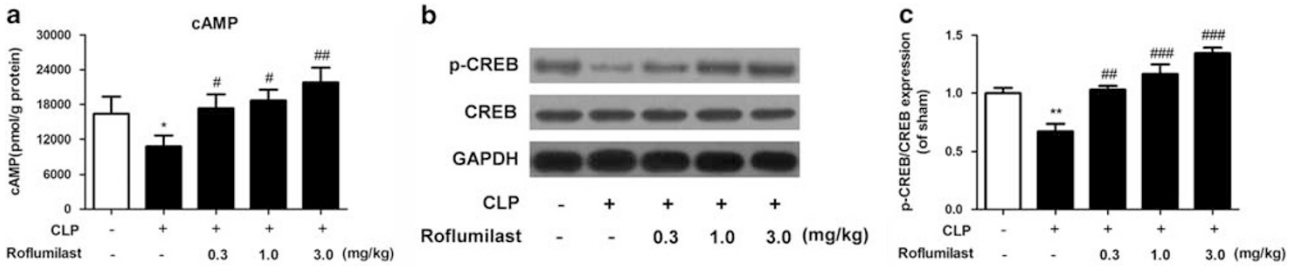

Figure 4 Roflumilast elevated the cAMP accumulation and CREB phosphorylation in CLP-induced sepsis. (**a**) Mice were subjected to CLP or sham operation. Sham group, $n=6$; other groups, $n=12$. Livers were collected 24 h after surgery. The levels of cAMP were determined using Mouse/Rat cAMP Parameter Assay Kit. Data were expressed as mean ± s.e.m. and compared using ANOVA. (**b**) Livers were collected 24 h after CLP or sham operation. The expression of phosphorylated CREB was determined by western blot. (**c**) The relative levels of phospho-CREB *vs* total CREB were determined by densitometry of the blots. Data were expressed as mean ± s.e.m. of three independent experiments and compared using ANOVA. $^{*}P<0.05$, $^{**}P<0.01$, compared with sham group; $^{\#\#}P<0.01$, $^{\#\#\#}P<0.001$, compared with CLP group.

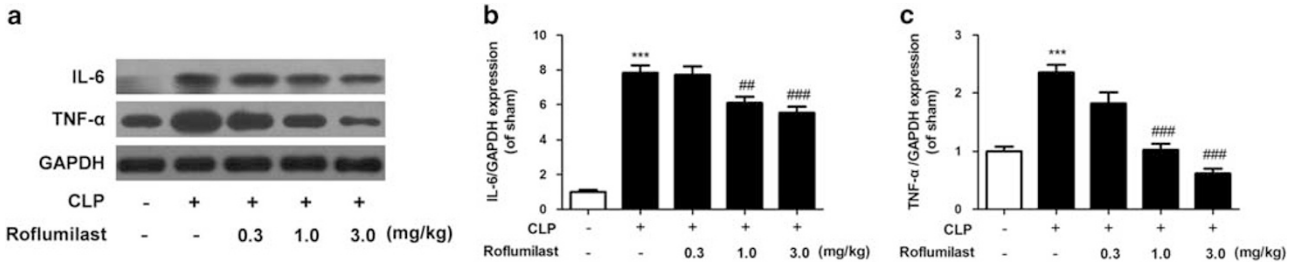

Figure 5 Roflumilast inhibited the expression of IL-6 and TNF-*α* in CLP-induced sepsis. (**a**) Livers were collected 24 h after CLP or sham operation. The expression of IL-6 and TNF-*α* was determined by western blot. (**b**) The relative levels of IL-6 *vs* GAPDH and (**c**) TNF-*α* *vs* GAPDH were determined by densitometry. Data were expressed as mean ± s.e.m. of three independent experiments and compared using ANOVA. $^{***}P<0.001$, compared with sham group; $^{\#\#}P<0.01$, $^{\#\#\#}P<0.001$, compared with CLP group.

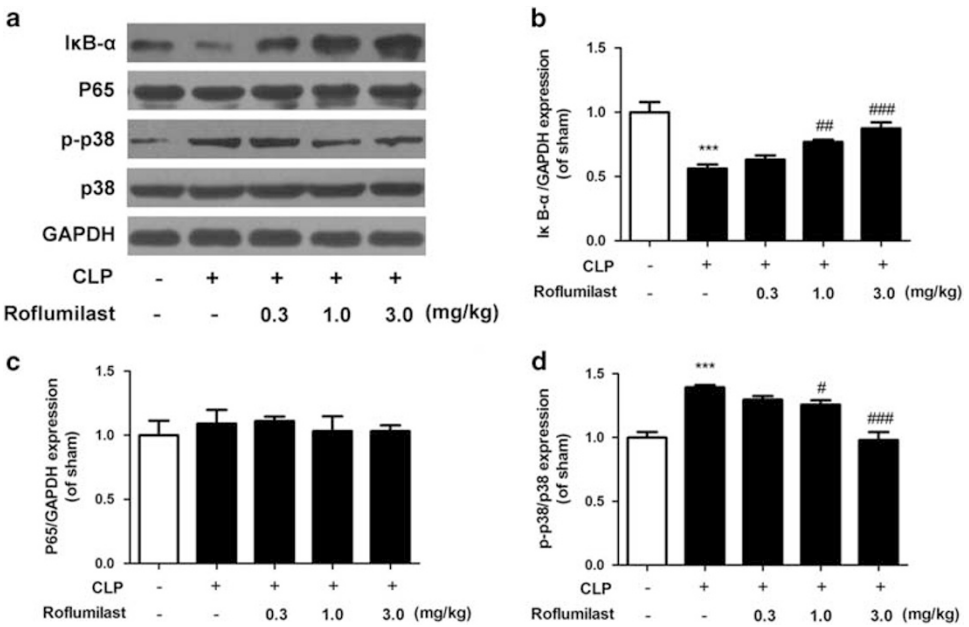

Figure 6 Roflumilast inhibited IκB degradation and p38 MAPK phosphorylation in CLP-induced sepsis. (**a**) Livers were collected 24 h after CLP or sham operation. The expression of Iκ*B*-*α*, NF-κB p65, and phosphorylated p38 was determined by western blot. (**b**) The relative levels of Iκ*B*-α *vs* GAPDH and (**c**) NF-κB p65 *vs* GAPDH were determined by densitometry. (**d**) The relative levels of phospho-p38 *vs* total p38 were determined by densitometry. Data were expressed as mean ± s.e.m. of three independent experiments and compared using ANOVA. $^{***}P<0.001$, compared with sham group; $^{\#}P<0.05$, $^{\#\#}P<0.01$, $^{\#\#\#}P<0.001$, compared with CLP group.

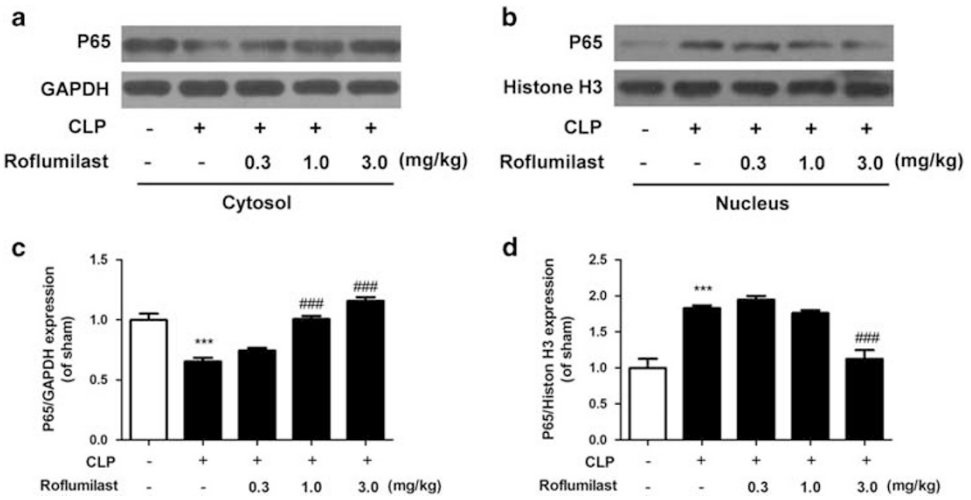

Figure 7 Roflumilast inhibited the nuclear translocation of NF-κB in CLP-induced sepsis. (**a**, **c**) Livers were excised 24 h after CLP or sham operation, and subcellular fractionation was extracted. The expression of NF-κB p65 in cytoplasmic and nuclear fractions was determined by western blot. (**b**, **d**) The relative levels of NF-κB p65 *vs* GAPDH or Histone H3 were determined by densitometry. GAPDH was used for the cytoplasmic fraction, while Histone H3 was used for the nuclear fraction. Data were expressed as mean ± s.e.m. of three independent experiments and compared using ANOVA. ***$P<0.001$, compared with sham group; $^{###}P<0.001$, compared with CLP group.

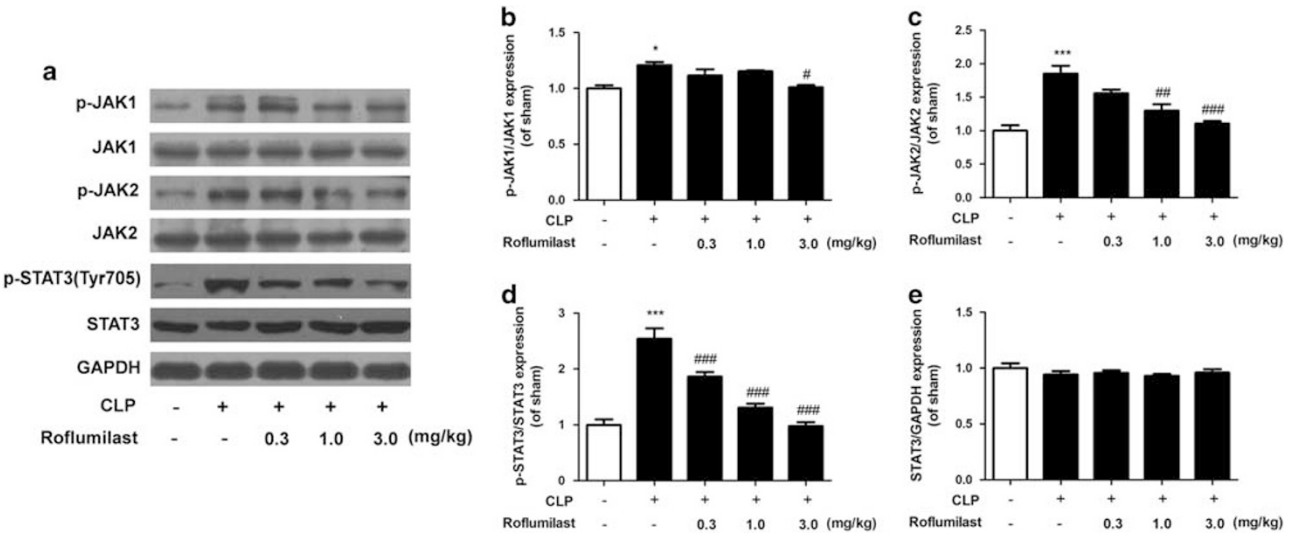

Figure 8 Roflumilast inhibited STAT3 pathway in CLP-induced sepsis. (**a**) Livers were collected 24 h after CLP or sham operation. The expression of phosphorylated STAT3, JAK1, and JAK2 was determined by western blot. (**b**) The relative levels of phospho-JAK1 *vs* total JAK1, (**c**) phospho-JAK2 *vs* total JAK2, and (**d**) phospho-STAT3 *vs* total STAT3 were determined by densitometry. Data were expressed as mean ± s.e.m. of three independent experiments and compared using ANOVA. *$P<0.05$, ***$P<0.001$, compared with sham group; $^{#}P<0.05$, $^{##}P<0.01$, $^{###}P<0.001$, compared with CLP group.

JAK2 phosphorylation. Furthermore, we investigated the role of roflumilast in STAT3 nuclear translocation. Our data showed that CLP enhanced STAT3 nuclear translocation, which was reversed by roflumilast treatment (Figures 9a–d).

DISCUSSION

Our study demonstrated the therapeutic potential of roflumilast in CLP-induced sepsis, using a realistic model of human sepsis.[40,41] Specifically, we demonstrated that roflumilast treatment improved the survival of septic mice by ameliorating the pathogenesis of sepsis as follows: (1) reduction of bacterial load locally and systemically; (2) suppression of cytokine production; (3) alleviation of liver injury; (4) inhibition of NF-κB and p38 MAPK signaling; and (5) inhibition of STAT3 signaling.

Roflumilast is a potent and selective PDE4 inhibitor. It decreases inflammatory response in several disease models. In bacterial-derived COPD model, roflumilast treatment reduced leukocyte infiltration to lung, inhibited lung inflammation, and prevented liver injury, including small airway wall remodeling and emphysema.[42] Roflumilast also reduced serum levels of pro-inflammatory cytokines in COPD

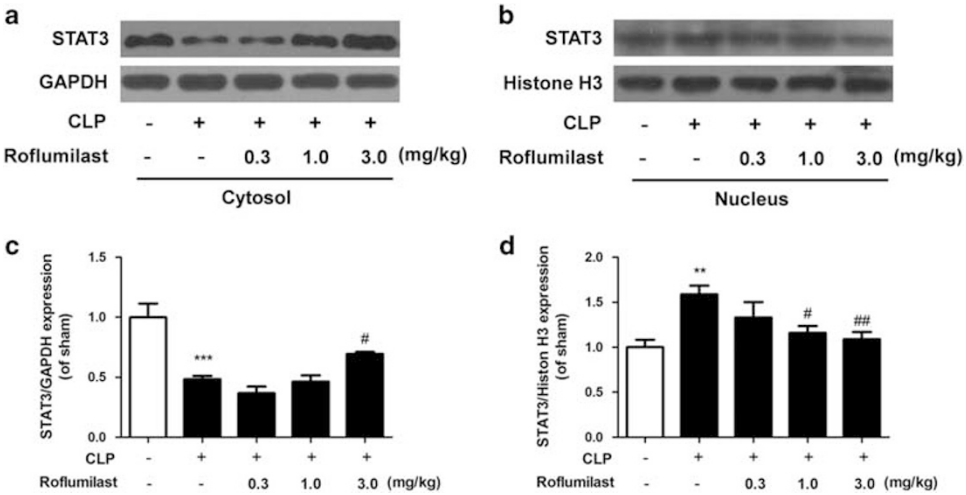

Figure 9 Roflumilast inhibited the nuclear translocation of STAT3 in CLP-induced sepsis. (**a**, **c**) Livers were excised 24 h after CLP or sham operation, and subcellular fractions were extracted. The expression of STAT3 in cytoplasmic and nuclear fractions was determined using western blot. (**b**, **d**) The relative levels of STAT3 *vs* GAPDH or Histone H3 were determined by densitometry. GAPDH was used for the cytoplasmic fraction, while Histone H3 was used for the nuclear fraction. Data were expressed as mean ± s.e.m. of three independent experiments and compared using ANOVA. $^{**}P<0.01$, $^{***}P<0.001$, compared with sham group; $^{\#}P<0.05$, $^{\#\#}P<0.01$, compared with CLP group.

patients.[43] Moreover, a preclinical study showed that roflumilast was effective to attenuate systemic inflammation and increase survival in mice exposed to LPS.[44] Here we also observed that roflumilast treatment inhibited the elevation of pro-inflammatory cytokines TNF-α and IL-6 in septic mice, which are responsible for the overwhelming inflammatory response. Roflumilast treatment also improved the survival of septic mice and reduced the bacterial load, the original stimulus in sepsis, indicating a better outcome. Roflumilast treatment exhibits therapeutic effects on CLP-induced sepsis.

Another important finding in our study is that roflumilast prevented liver inflammation and liver injury in septic mice. The protective effect of roflumilast against liver injury has never been reported. Owing to the complex physiological mechanisms associated with host defense and immunological homeostasis, liver is significantly affected and has a prominent role in sepsis.[45,46] A clinico-pathological study has reported that histology of liver biopsy specimens of patients dying from sepsis typically showed inflammation, necrosis, hepatocellular steatosis, and apoptosis. Levels of ALT and AST, indicators of hepatocellular damage, were increased in patients before death.[47] Similar biochemical and histological changes were reproduced in septic mice induced by CLP,[32,33] which was also shown in our results. The mechanisms of liver injury in sepsis are complex and involve the interaction of multiple pathophysiological processes. Recent studies indicates that liver injury in sepsis is mainly resulted from excessive generation of inflammation mediators.[14,48] In sepsis, liver cells, Kupffer cells particularly, are activated by spillover of microbial factors. Activated Kupffer cells produced excessive inflammatory mediators such as IL-1, IL-6 and TNF-α, nitric oxide, and reactive oxygen species. These mediators are either released into systemic circulation mediating multi-organ injury, or interact with hepatocytes and sinusoidal endothelial cells via paracrine mediating hepatic injury.[46] It has been shown that suppression of liver inflammation attenuated the liver injury, decreasing morbidity and mortality of sepsis.[49] Decreased levels of IL-6 and TNF-α in liver were also shown in roflumilast treatment groups, accompanied with the alleviation of liver injury. The mechanisms by which roflumilast inhibited liver inflammation and liver injury were also investigated.

As an inhibitor of PDE4, roflumilast raises the intracellular levels of cAMP. Increased cAMP activates PKA, which in turn activates CREB, a transcription factor that regulates the expression of numerous genes.[22,23] It was shown that activation of cAMP–CREB pathway inhibited the generation of pro-inflammation cytokines.[22] Consistent with the ELISA data, western blot results confirmed that levels of IL-6 and TNF-α in septic livers were decreased by roflumilast. Notably, we observed that sepsis induction by CLP resulted in reduced cAMP and phosphorylated CREB in liver, indicating a potential role of cAMP–CREB pathway in the pathogenesis of sepsis. Roflumilast treatment upregulated the reduction of cAMP and phosphorylated CREB suggesting the efficacy of roflumilast in sepsis-induced liver injury. These results indicated that roflumilast is effective to suppress liver inflammation via activation of cAMP–CREB pathway.

Studies previously demonstrated the role of TLRs in the production of cytokines and activation of inflammatory cascades in sepsis.[15,35,50] After microbial factors and endogenous inflammatory agonists bind their cognate TLR receptors, TLR dimers initiate intracellular signaling cascades via sequential phosphorylation of kinases such as p38 MAPK, inducing the activation of transcription factors NF-κB and

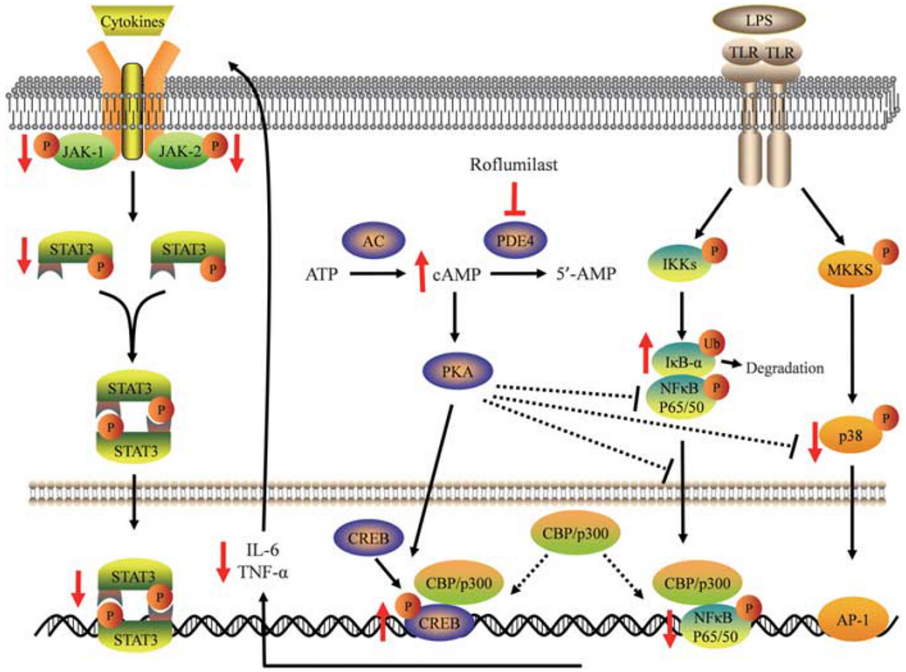

Figure 10 Roflumilast inhibited NF-κB and STAT3 signals in CLP-induced sepsis. After microbial factors bind to cognate TLR receptors in sepsis, TLR dimers activate intracellular NF-κB signaling cascades. Activation of NF-κB correlates with ubiquitination and degradation of the NF-κB inhibitor IκB-α, resulting in the dissociation of NF-κB. Liberated NF-κB sequentially translocates to the nucleus where it initiates transcription of immune-related genes such as IL-6 and TNF-α. Moreover, TLR dimers also phosphorylate p38 MAPK, inducing activation of transcription factor AP-1, facilitating transcription of cytokines. Cytokines exhibit their biological effects through activation of STAT3, which occurs via phosphorylation of JAK1, JAK2, and STAT3. Phosphorylated STAT3 dimerizes and translocates to the nucleus, initiating transcription of target genes. Roflumilast regulated NF-κB and p38 MAPK signaling by suppression of IκB-α degradation, NF-κB translocation, and p38 MAPK phosphorylation, thereby inhibiting consequent production of cytokines and cytokine-mediated activation of STAT3. On the other hand, roflumilast increased cAMP accumulation and CREB phosphorylation. Activation of CREB is potentially involved in the inhibition of NF-κB and p38 MAPK signaling.

AP-1.[15,16] However, there is limited information on the role of NF-κB signaling in sepsis-induced liver injury. Our results showed that the degradation of IκB-α and accumulation of NF-κB in the nucleus were increased in septic mice, indicating the involvement of NF-κB in sepsis-induced liver injury. Interestingly, roflumilast significantly reversed these changes. Moreover, consistent with previous studies,[16] the phosphorylation of p38 MAPK was increased in the liver after CLP, which was inhibited by roflumilast. Our study introduced NF-κB and p38 MAPK into the field of sepsis-induced liver injury, and here we linked the changes of NF-κB and p38 MAPK to PDE4, as roflumilast is a PDE4 inhibitor. Previous reports showed that the activation of NF-κB could be inhibited by cAMP–CREB signaling, probably due to the competition between CREB and NF-κB for the limited amounts of cofactor CBP,[51] via the inhibition of NF-κB nuclear translocation by PKA,[52] or via direct or indirect modification of the C-terminal transactivation domain of the NF-κB p65.[53] Furthermore, cAMP also affected p38 MAPK activation.[54] Interferon gamma- and TNF-α-induced p38 MAPK phosphorylation was significantly suppressed by cAMP-dependent PKA activity in HaCaT cells.[55] These results suggested that roflumilast suppresses liver inflammation probably via inhibition of NF-κB and p38 MAPK signaling.

The STAT signaling is another essential pathway in cytokine production. STATs are triggered by microbial factors during sepsis.[20] In addition, the STAT signaling is activated in response to cytokine stimulation, mediating the signal transduction of cytokines.[56,57] Activated STATs dimerize and translocate to the nucleus, where they bind to specific promoter sequences and induce transcription of target genes. STAT3 is a key transcription factor in both immune and inflammatory pathways. LPS enhanced the expression of STAT3 and subsequent generation of TNF-α and IL-1β.[58] STAT3 was also activated in response to various cytokines such as IL-6 and TNF-α.[57] Interestingly, STAT3 activation may result in increased IL-6 expression, which in turn induces STAT3 phosphorylation and regulates diverse biological responses subsequently.[59] However, the role of STAT3 signaling in sepsis-induced liver injury remains largely unclear. The activated STAT3 signaling in septic livers in this study is in harmony with a recent study that observed increased phosphorylated STAT3 in liver from septic mice,[60] indicating a potential role of STAT3 signaling in the pathogenesis of sepsis. It is quite interesting that roflumilast treatment inhibited the phosphorylation and nucleus accumulation of STAT3, as well as the phosphorylation of upstream JAK1 and JAK2. These results suggested that

inhibition of STAT3 signaling may have a vital role in alleviating liver injury of sepsis.

The recommended dosage of roflumilast for patients with COPD is 500 μg/day. In the present study, we found that roflumilast protected mice against CLP-induced sepsis in a dose-dependent manner, which reached a statistically significant level at 1.0 mg/kg. Notably, 1.0 mg/kg of roflumilast in mice is equivalent to 0.08 mg/kg of that in human according to 'Conversion of Animal Doses to Human Equivalent Doses' from the US FDA.[61] Although 1–10 mg/kg of roflumilast is a common dosage regime used in animal studies,[62–64] we still need to point out that the minimal effective dose of roflumilast in this study is about 10 times higher than the recommended dosage used in human for COPD. We speculate the high doses roflumilast needed in sepsis may be due to the rapidly progression and severity of sepsis and the shorter-term treatment than COPD. Nevertheless, additional studies to further evaluate the safety and possible side effects of roflumilast at 1.0 mg/kg are required in the future.

In the current study, we used the CLP model to test the effect of roflumilast on sepsis-induced liver injury. Notably, using only one model in the study is not yet adequate to support our hypothesis that roflumilast could protect mice against sepsis-induced liver injury. Further studies in other models are need to confirm our findings. Moreover, in the present study, we found that roflumilast enhanced the level of cAMP and activated PKA/CREB signaling pathway in the liver in our model. However, as there are crosstalk between PKA/CREB signaling and other signal pathways, such as MKK/p38 MAPK and IKK/NF-κB pathways, more studies are still needed to elucidate the interaction between these pathways and the exact mechanisms by which roflumilast reduces inflammation in sepsis. Notwithstanding the limitations, this study does introduce roflumilast into the field of sepsis-induced liver injury. In addition, as sepsis is a systemic disease and PDE4 is widely expressed throughout the body, the protective effect of roflumilast might not be confined to liver injury.

In summary, these results indicate for the first time that treatment with the PDE4 inhibitor roflumilast is an effective strategy against CLP-induced sepsis. Roflumilast suppressed the expression of pro-inflammatory cytokines IL-6 and TNF-α, alleviated liver damage, and improved survival in polymicrobial sepsis, probably via blockade of the NF-κB, p38 MAPK, and STAT3 pathways (Figure 10). The current data provide novel insights into the pharmacological activities of roflumilast as an add-on strategy for the treatment of sepsis.

ACKNOWLEDGMENTS

This work was supported by National Natural Science Fund of China (Nos. 81373384 and 81503043) and Funding from Guangdong Science and Technology Department (Nos. 2012B050500005 and 2015B020211007).

DISCLOSURE/CONFLICT OF INTEREST

The authors declare no conflict of interest.

1. Singer M, Deutschman CS, Seymour CW, *et al.* The Third International Consensus Definitions for Sepsis and Septic Shock (Sepsis-3). JAMA 2016;315:801–810.
2. Dellinger RP, Levy MM, Rhodes A, *et al.* Surviving Sepsis Campaign: international guidelines for management of severe sepsis and septic shock, 2012. Crit Care Med 2013;41:580–637.
3. Vincent JL, Marshall JC, Ñamendys-Silva SA, *et al.* Assessment of the worldwide burden of critical illness: the Intensive Care Over Nations (ICON) audit. Lancet Respir Med 2014;2:380–386.
4. Mayr FB, Yende S, Angus DC. Epidemiology of severe sepsis. Virulence 2014;5:4–11.
5. Adhikari NKJ, Fowler RA, Bhagwanjee S, *et al.* Critical care and the global burden of critical illness in adults. Lancet 2010;376:1339–1346.
6. Torio CM, Moore BJ. Healthcare Cost and Utilization Project (HCUP) Statistical Briefs. Rockville (MD): Agency for Healthcare Research and Quality (US). National inpatient hospital costs: the most expensive conditions by payer, 2013: statistical brief #204. Available from: https://www.hcup-us.ahrq.gov/reports/statbriefs/sb204-Most-Expensive-Hospital-Conditions.jsp. Accessed on April 22, 2017.
7. Martin-Loeches I, Levy MM, Artigas A. Management of severe sepsis: advances, challenges, and current status. Drug Des Devel Ther 2015;9:2079–2088.
8. Nesseler N, Launey Y, Aninat C, *et al.* Clinical review: the liver in sepsis. Crit Care 2012;16:235.
9. Tsai TN, Ho JJ, Liu MS, *et al.* Role of exogenous Hsp72 on liver dysfunction during sepsis. Biomed Res Int 2015;2015:508101.
10. Vincent JL, Angus DC, Artigas A, *et al.* Effects of drotrecogin alfa (activated) on organ dysfunction in the PROWESS trial. Crit Care Med 2003;31:834–840.
11. Brun-Buisson C, Meshaka P, Pinton P, *et al.* EPISEPSIS: a reappraisal of the epidemiology and outcome of severe sepsis in French intensive care units. Intensive Care Med 2004;30:580–588.
12. Jekarl DW, Kim JY, Lee S, *et al.* Diagnosis and evaluation of severity of sepsis via the use of biomarkers and profiles of 13 cytokines: a multiplex analysis. Clin Chem Lab Med 2015;53:575–581.
13. Toscano MG, Ganea D, Gamero AM. Cecal ligation puncture procedure. J Vis Exp 2011;51:2860.
14. Abraham E, Singer M. Mechanisms of sepsis-induced organ dysfunction. Crit Care Med 2007;35:2408–2416.
15. Khakpour S, Wilhelmsen K, Hellman J. Vascular endothelial cell Toll-like receptor pathways in sepsis. Innate Immun 2015;21:827–846.
16. Liang YJ, Li X, Zhang XJ, *et al.* Elevated levels of plasma TNF-α are associated with microvascular endothelial dysfunction in patients with sepsis through activating the NF-κB and p38 mitogen-activated protein kinase in endothelial cells. Shock 2014;41:275–281.
17. Bohrer H, Qiu F, Zimmermann T, *et al.* Role of NFkappaB in the mortality of sepsis. J Clin Invest 1997;100:972–985.
18. McKenna S, Gossling M, Bugarini A, *et al.* Endotoxemia induces IκBβ/NF-κB-dependent endothelin-1 expression in hepatic macrophages. J Immunol 2015;195:3866–3879.
19. Higuchi Y, Kawakami S, Yamashita F, *et al.* The potential role of fucosylated cationic liposome/NFkappaB decoy complexes in the treatment of cytokine-related liver disease. Biomaterials 2007;28:532–539.
20. Lv X, Zhang Y, Cui Y, *et al.* Inhibition of microRNA-155 relieves sepsis induced liver injury through inactivating the JAK/STAT pathway. Mol Med Rep 2015;12:6013–6018.
21. Hui L, Yao Y, Wang S, *et al.* Inhibition of Janus kinase 2 and signal transduction and activator of transcription 3 protect against cecal ligation and puncture-induced multiple organ damage and mortality. J Trauma 2009;66:859–865.
22. Raker VK, Becker C, Steinbrink K. The cAMP pathway as therapeutic target in autoimmune and inflammatory diseases. Front Immunol 2016;7:123.
23. Yan K, Gao LN, Cui YL, *et al.* The cyclic AMP signaling pathway: exploring targets for successful drug discovery (Review). Mol Med Rep 2016;13:3715–3723.
24. Gobejishvili L, Barve S, Breitkopf-Heinlein K, *et al.* Rolipram attenuates bile duct ligation-induced liver injury in rats: a potential pathogenic role of PDE4. J Pharmacol Exp Ther 2013;347:80–90.

25. Gobejishvili L, Barve S, Joshi-Barve S, *et al.* Enhanced PDE4B expression augments LPS-inducible TNF expression in ethanol-primed monocytes: relevance to alcoholic liver disease. Am J Physiol Gastrointest Liver Physiol 2008;295:G718–G724.
26. Gantner F, Küsters S, Wendel A, *et al.* Protection from T cell-mediated murine liver failure by phosphodiesterase inhibitors. J Pharmacol Exp Ther 1996;280:53–60.
27. Fabbri LM, Beghe B, Yasothan U, *et al.* Roflumilast. Nat Rev Drug Discov 2010;9:761–762.
28. Ulrik CS, Calverley PM. Roflumilast: clinical benefit in patients suffering from COPD. Clin Respir J 2010;4:197–201.
29. Rittirsch D, Huber-Lang MS, Flierl MA, *et al.* Immunodesign of experimental sepsis by cecal ligation and puncture. Nat Protoc 2009;4:31–36.
30. Shrum B, Anantha RV, Xu SX, *et al.* A robust scoring system to evaluate sepsis severity in an animal model. BMC Res Notes 2014;7:233.
31. Weber GF, Chousterman BG, He S, *et al.* Interleukin-3 amplifies acute inflammation and is a potential therapeutic target in sepsis. Science 2015;347:1260–1265.
32. Liang D, Hou Y, Lou X, *et al.* Decoy receptor 3 improves survival in experimental sepsis by suppressing the inflammatory response and lymphocyte apoptosis. PLoS ONE 2015;10:e131680.
33. Martin EL, Souza DG, Fagundes CT, *et al.* Phosphoinositide-3 kinase gamma activity contributes to sepsis and organ damage by altering neutrophil recruitment. Am J Respir Crit Care Med 2010;182:762–773.
34. Susuki-Miyata S, Miyata M, Lee BC, *et al.* Cross-talk between PKA-Cβ and p65 mediates synergistic induction of PDE4B by roflumilast and NTHi. Proc Natl Acad Sci USA 2015;114:E1800–E1809.
35. Kumar S, Ingle H, Prasad DV, *et al.* Recognition of bacterial infection by innate immune sensors. Crit Rev Microbiol 2013;39:229–246.
36. Ulloa L, Tracey KJ. The "cytokine profile": a code for sepsis. Trends Mol Med 2005;11:56–63.
37. Abraham E. Nuclear factor-kappaB and its role in sepsis-associated organ failure. J Infect Dis 2003;187:S364–S369.
38. Levy Jr. DE, Darnell JE. Stats: transcriptional control and biological impact. Nat Rev Mol Cell Biol 2002;3:651–662.
39. Shuai K, Liu B. Regulation of JAK-STAT signalling in the immune system. Nat Rev Immunol 2003;3:900–911.
40. Ward PA. New approaches to the study of sepsis. EMBO Mol Med 2012;4:1234–1243.
41. Buras JA, Holzmann B, Sitkovsky M. Animal models of sepsis: setting the stage. Nat Rev Drug Discov 2005;4:854–865.
42. Richmond BW, Brucker RM, Han W, *et al.* Airway bacteria drive a progressive COPD-like phenotype in mice with polymeric immunoglobulin receptor deficiency. Nat Commun 2016;7:11240.
43. Grootendorst DC, Gauw SA, Verhoosel RM, *et al.* Reduction in sputum neutrophil and eosinophil numbers by the PDE4 inhibitor roflumilast in patients with COPD. Thorax 2007;62:1081–1087.
44. Schick MA, Wunder C, Wollborn J, *et al.* Phosphodiesterase-4 inhibition as a therapeutic approach to treat capillary leakage in systemic inflammation. J Physiol 2012;590:2693–2708.
45. Yan J, Li S, Li S. The role of the liver in sepsis. Int Rev Immunol 2014;33:498–510.
46. Dhainaut JF, Marin N, Mignon A, *et al.* Hepatic response to sepsis: interaction between coagulation and inflammatory processes. Crit Care Med 2001;29:S42–S47.
47. Koskinas J. Liver histology in ICU patients dying from sepsis: a clinico-pathological study. World J Gastroenterol 2008;14:1389.
48. Jean-Baptiste E. Cellular mechanisms in sepsis. J Intensive Care Med 2007;22:63–72.
49. Liu A, Wang W, Fang H, *et al.* Baicalein protects against polymicrobial sepsis-induced liver injury via inhibition of inflammation and apoptosis in mice. Eur J Pharmacol 2015;748:45–53.
50. Weighardt H, Holzmann B. Role of Toll-like receptor responses for sepsis pathogenesis. Immunobiology 2007;212:715–722.
51. Parry GC, Mackman N. Role of cyclic AMP response element-binding protein in cyclic AMP inhibition of NF-kappaB-mediated transcription. J Immunol 1997;159:5450–5456.
52. King CC, Sastri M, Chang P, *et al.* The rate of NF-kappaB nuclear translocation is regulated by PKA and A kinase interacting protein 1. PLoS ONE 2011;6:e18713.
53. Takahashi N, Tetsuka T, Uranishi H, *et al.* Inhibition of the NF-kappaB transcriptional activity by protein kinase A. Eur J Biochem 2002;269:4559–4565.
54. Korhonen R, Hommo T, Keranen T, *et al.* Attenuation of TNF production and experimentally induced inflammation by PDE4 inhibitor rolipram is mediated by MAPK phosphatase-1. Br J Pharmacol 2013;169:1525–1536.
55. Qi XF, Kim DH, Yoon YS, *et al.* The adenylyl cyclase-cAMP system suppresses TARC/CCL17 and MDC/CCL22 production through p38 MAPK and NF-kappaB in HaCaT keratinocytes. Mol Immunol 2009;46:1925–1934.
56. Guo L, Junttila IS, Paul WE. Cytokine-induced cytokine production by conventional and innate lymphoid cells. Trends Immunol 2012;33:598–606.
57. De Simone V, Franze E, Ronchetti G, *et al.* Th17-type cytokines, IL-6 and TNF-α synergistically activate STAT3 and NF-κB to promote colorectal cancer cell growth. Oncogene 2015;34:3493–3503.
58. Yang P, Li Z, Li H, *et al.* Pyruvate kinase M2 accelerates pro-inflammatory cytokine secretion and cell proliferation induced by lipopolysaccharide in colorectal cancer. Cell Signal 2015;27:1525–1532.
59. Fielding CA, McLoughlin RM, McLeod L, *et al.* IL-6 regulates neutrophil trafficking during acute inflammation via STAT3. J Immunol 2008;181:2189–2195.
60. Hutchins NA, Wang F, Wang Y, *et al.* Kupffer cells potentiate liver sinusoidal endothelial cell injury in sepsis by ligating programmed cell death ligand-1. J Leukoc Biol 2013;94:963–970.
61. U.S. Food and Drug Administration. Guidance for industry: estimating the maximum safe starting dose in initial clinical trials for therapeutics in adult healthy volunteers. Rockville, Maryland. 2005. Available at https://www.fda.gov/downloads/drugs/guidancecomplianceregulatoryinformation/guidances/ucm078932.pdf. Accessed on April 22, 2017.
62. Hatzelmann A, Morcillo EJ, Lungarella G, *et al.* The preclinical pharmacology of roflumilast—a selective, oral phosphodiesterase 4 inhibitor in development for chronic obstructive pulmonary disease. Pulm Pharmacol Ther 2010;23:235–256.
63. Aldrich A, Bosch ME, Fallet R, *et al.* Efficacy of phosphodiesterase-4 inhibitors in juvenile Batten disease (CLN3). Ann Neurol 2016;80:909–923.
64. Koga H, Recke A, Vidarsson G, *et al.* PDE4 inhibition as potential treatment of epidermolysis bullosa acquisita. J Invest Dermatol 2016;136:2211–2220.